Structure, stability, and infrared spectroscopy of $(H_2O)_n NH_4^+$ clusters: A theoretical study at zero and finite temperature

Cite as: J. Chem. Phys. **129**, 154305 (2008); https://doi.org/10.1063/1.2987304
Submitted: 13 June 2008 . Accepted: 27 August 2008 . Published Online: 16 October 2008

J. Douady, F. Calvo, and F. Spiegelman

Structure, stability, and infrared spectroscopy of $(H_2O)_nNH_4^+$ clusters: A theoretical study at zero and finite temperature

J. Douady,[1] F. Calvo,[2,a)] and F. Spiegelman[1]
[1]*LCPQ, IRSAMC, Université Paul Sabatier, 118 Route de Narbonne, F31062 Toulouse Cedex, France*
[2]*LASIM, Université Claude Bernard Lyon 1, Bât. A. Kastler, 43 Bd du 11 Novembre 1918, F69622 Villeurbanne, France*

(Received 13 June 2008; accepted 27 August 2008; published online 16 October 2008)

The combined effects of size and temperature on the stable structures of water clusters doped with one ammonium molecule have been investigated theoretically using an empirical potential and density-functional theory (DFT) calculations. Global optimization with Monte Carlo methods has been performed using an explicit intermolecular potential based on the Kozack–Jordan polarizable model. Putative lowest-energy structures based on this empirical potential are reported. Our results indicate a high propensity for the NH_4^+ impurity to be fully solvated by water molecules. Clathratelike patterns are formed for clusters containing more than 11 molecules. Local reoptimizations of candidate structures carried out at the DFT level with the B3LYP hybrid functional and the 6-311++G(d,p) basis set confirm the general trends obtained with the intermolecular potential. However, some reorderings between isomers often due to zero-point energy corrections are found in small clusters, leading to stable geometries in agreement with other first-principles studies. Temperature effects have been assessed using a simple harmonic superposition approximation for selected cluster sizes and using dedicated Monte Carlo simulations for $(H_2O)_{20}NH_4^+$. The clusters are found to melt near 200 K, and possibly isomerize already below 50 K. The free energy barrier for core/surface isomerization of the impurity in the 21-molecule cluster is estimated to be only a few kcal/mol at 150 K. The vibrational spectroscopic signatures of the clusters obtained from the electronic structure calculations show the usual four O–H stretching bands. As the cluster size increases, the double acceptor-single donor band near 3700 cm^{-1} increasingly dominates over the three other bands. While we do not find conclusive evidence for a O–H stretching spectroscopic signature of the ammonium impurity to be in the core or at the surface in the 20-molecule cluster, a possible signature via the N–H stretching bands is suggested near 2800–2900 cm^{-1}. In the larger $(H_2O)_{49}NH_4^+$ cluster, the impurity is slightly more stable at the surface. © *2008 American Institute of Physics*. [DOI: 10.1063/1.2987304]

I. INTRODUCTION

Protonated water complexes are key elements to dissociation and transport phenomena in aqueous chemistry and biological systems. In addition to their fundamental chemical relevance, protonated water clusters play an important role in a number of areas, including atmospheric sciences,[1–6] astrophysics,[7] and biology.[8] It is therefore not a surprise that protonated water clusters have received extensive attention from both the experimental and theoretical communities during the past decades. Early experiments focused primarily on the binding energies and relative abundances of $(H_2O)_nH^+$ clusters of different sizes, especially near the magic number $n=21$.[9–11] After years of investigations and relative controversy, there is now general agreement about the cage structure of this cluster, the extra proton being more likely located at the surface.[12–18]

From a theoretical point of view, the study of protonated water clusters faces two main challenges. First, water clusters have a very complicated energy landscape consisting of many competing structures.[19] This was suggested by several studies at various levels of electronic structure theory,[20–24] but became clearer after the sampling issue could be tackled using empirical potentials.[25–31] For instance, graph theory indicates that more than 30 000 symmetry-distinct hydrogen bond topologies can be found for the $(H_2O)_{20}$ cluster with dodecahedral arrangement of oxygen atoms, providing as many likely candidates as local minimum structures.[32] More specific to the case of protonated clusters, a second difficulty lies in the numerous bonding sites of the extra proton, and the possible formation of Zundel[33] complexes.

Neutral water clusters doped with an ammonium molecule are also convenient for size selection in experimental measurements. Small $(H_2O)_nNH_4^+$ clusters, $n=1-6$, have been studied by vibrational predissociation spectroscopy[34–36] aimed at determining the stable structures. In larger clusters, magic numbers have been reported[37,38] to occur at $n=20$ and $n=27$ and, more recently,[39] at $n=52$ and 54. This shift of one water molecule with respect to $(H_2O)_nH^+$ clusters was interpreted as the likely replacement of the hydronium ion by NH_4^+ in the protonated water cluster, hence sharing its structural features.

While the extra proton can be delocalized in protonated

a)Electronic mail: fcalvo@lasim.univ-lyonl.fr.

water clusters, it is expected to be essentially localized on the ammonium molecule, reflecting its higher proton affinity of 204 kcal/mol versus only 165 kcal/mol for water.[40,41] Despite showing simpler chemistry, water clusters doped by a single ammonium impurity have been comparatively poorly investigated except at small sizes and near the magic number $n=20$. At semi-empirical,[42] Hartree–Fock and post-Hartree–Fock levels,[43–53] several authors looked for the stable structures and solvation properties of $(H_2O)_n(NH_3)H^+$ with $n=1-6$. More recently, density-functional theory (DFT) calculations have been performed as well.[36,38,54–56] These works generally confirmed the preferred location of the proton on the ammonia molecule rather than on any of the water molecules, and indicated that isomers appear at size $n=4$. The calculated vibrational spectra of these small species, usually obtained from static geometries but also from explicit molecular dynamics trajectories[53] have now reached agreement with experimentally available measurements.[34–36]

Concerning larger $(H_2O)_nNH_4^+$ clusters, Khan[57] investigated the case $n=20$ in dodecahedral cage configurations using *ab initio* calculations at the Hartree–Fock, MP2, and DFT levels. This study concluded that the core and surface bonding sites of the ammonium molecule in this cluster are very close in energy. However, it should be noted that all surface molecules in the structures considered by this author have a dangling OH bond, making them rather unrealistic. Based on quantum chemical calculations and on comparison with spectroscopic measurements, Diken *et al.*[38] found preferential attachment of the ammonium at the surface of the 20-molecule cluster. More recently, the DFT calculations performed by Schmidt *et al.*[39] supported this more stable surface location of NH_4^+.

Because they relied on an explicit treatment of electronic structure, the aforementioned studies have not attempted a systematic and unbiased search of the stable configurations of $(H_2O)_nNH_4^+$ clusters, especially at sizes away from magic numbers. Despite the development of increasingly sophisticated electronic structure methods to describe interactions in aqueous media,[58] efficient sampling can only be addressed by simpler models. Explicit, classical potentials are thus invaluable for surveying the low-energy parts of the energy landscape, eventually refining the results at more sophisticated levels of theory.

Empirical potentials for the water-ammonium system have been mostly used for studying the rotation dynamics of NH_4^+ solvated in bulk water, known from NMR measurements to be fast.[59,60] The small barrier of about 2 kcal/mol involved in this rotation was initially met with some surprise because the shell of surrounding water molecules was thought to bind significantly with the ammonium ion. Several theoretical works have since then tried to tackle this problem using a variety of methods, paying a particular attention to the coordination of NH_4^+ at zero or finite temperature.[61–69] However, no general consensus has been reached so far from the computational side.

Our first objectives in the present article are to achieve global optimization of $(H_2O)_nNH_4^+$ clusters and to cover a broader size range than in previous work. For this global optimization task, we use a polarizable model inspired by previous potentials developed for water by Kozack and Jordan[70,71] (KJ) and for ammonium by Dang.[65] A unified potential is built here along the lines of the KJ potential, in which both H_2O and NH_4^+ molecules are modeled at the same level of complexity. This potential has been partly reparametrized based on the detailed DFT results obtained by Brugé *et al.*[66] on small $(H_2O)_nNH_4^+$ clusters, $n=1-5$.

Besides mass spectrometry, information on the structural properties of $(H_2O)_nNH_4^+$ clusters essentially originates from infrared spectroscopy measurements.[34–36,38] Recent progress in cooling techniques have led to significant improvements, allowing a much clearer geometrical characterization. As in the case of protonated water clusters,[12,13] variations in the stretching frequencies of dangling O–H bonds have been used to infer structural candidates.[72] We also trace here the possible structural signatures by computing vibrational spectra of $(H_2O)_nNH_4^+$ clusters using standard DFT. While our results generally agree with the measurements, they also suggest that the interpretation of O–H stretching bands may be ambiguous, preventing their use as a strong structural probe for medium-size clusters.

Two other aspects influence the stable structures of water clusters, namely, quantum vibrational delocalization and finite temperature. The numerous soft modes can lead to significant zero-point effects, as illustrated by Burnham *et al.*[73] on the water hexamer. In the case of $(H_2O)_nNH_4^+$ clusters, we show below that quantum nuclear effects also shuffle the ordering of the isomers. Temperature effects contribute to the broadening (and possible shifting) of infrared bands, but they can also affect the relative stabilities of the various isomers through changes in entropy. The thermodynamical properties of water clusters have been heavily investigated in the past, particularly with empirical models such as TIP4P (Refs. 25 and 74–77) and assuming classical statistical mechanics. Even though it has become possible to carry out finite-temperature studies of water using first-principle methods,[78,79] such simulations remain practically limited. Quantum statistics are another computational burden, and have been accounted for on very few occasions.[80–82] To get more insight into both quantum vibrations and finite-temperature effects on the stability of the smaller $(H_2O)_nNH_4^+$ clusters, we have used the harmonic superposition approximation,[19] previously employed in the classical case by Wales and Ohmine[25] for pure water clusters. Monte Carlo (MC) simulations using our empirical potential are also performed for the magic size $n=20$ to quantify the isomerization cost of the ammonium impurity for crossing between the surface and the core of the cluster.

The article is organized as follows. In Sec. II, we present the method chosen for the optimization problem, starting with our adaptation of the KJ water potential combined with the Dang model for the ammonium molecule. The global minimization results obtained for all clusters $(H_2O)_nNH_4^+$ $(1\leq n\leq 24)$ using this potential are then discussed. In Sec. III, the low-energy structures obtained with the empirical potential have been checked and refined using DFT minimizations with a hybrid functional and a large basis set. We also show that some structures are stabilized upon including zero-point effects. The influence of temperature on the structural

properties of $(H_2O)_nNH_4^+$ clusters is discussed in Sec. IV. In particular, we focus on the magic cluster $(H_2O)_{20}NH_4^+$ by emphasizing the role of the temperature on the ammonium mobility. Spectroscopic properties in the infrared domain are discussed in Sec. V for the smaller clusters $n \leq 21$. Section VI illustrates some results obtained for the structural properties of a larger cluster, $(H_2O)_{49}NH_4^+$. Finally, we briefly summarize and conclude in Sec. VII.

II. GLOBAL OPTIMIZATION

Our structural study relies on unbiased global optimization using an explicit intermolecular potential, aimed at sampling the low-energy regions of the potential energy landscape. The stable isomers are then refined using methods involving an explicit treatment of electronic structure. Because this work is a first part of a more general project on pure and doped water clusters, we have chosen a well established potential developed for water by Kozack and Jordan,[70] which was further extended for treating protonated water by the same authors.[71]

A. Polarizable potential

The KJ potential relies on a four-site rigid model for the water molecule, carrying four partial charges on the three atoms and an extra site M located on the symmetry axis toward the hydrogens. Two molecules interact via direct Coulomb forces, as well as repulsion-dispersion forces taken as a simple Lennard–Jones (LJ) form between the M sites. In addition, the KJ potential is polarizable and each site M is given a molecular polarizability of 1.47 Å^3, leading to explicit many-body interactions. The details of the KJ potential and the characteristics of the water molecule in this model can be found in the original reference.[70]

Consistently with the KJ model, a five-site rigid model was chosen to describe the ammonium impurity. The Dang potential developed for liquid phase simulations[65] provided a basis for our own potential. In this model, the nitrogen atom of the NH_4^+ molecule carries a LJ center interacting with the water sites M. Instead of the five atomic polarizable sites in the original Dang potential, a single molecular polarizability of 1.174 Å^3 was attributed to the nitrogen atom only.[65] The partial charges carried by the hydrogen and nitrogen atoms were taken as the original values of the Dang potential, namely, $q_H = +0.464$ and $q_N = -0.856$. The alteration in the polarization interactions lead us to adjust the LJ parameters. In this purpose the DFT calculations carried out by Brugé *et al.*[66] were used as a reference. A standard least-square fitting procedure provided the optimal LJ parameters σ and ε that best reproduce the hydration energies and the hydrogen bond distances between the ammonium hydrogens and the water oxygens in small $(H_2O)_nNH_4^+$ clusters, $n=1-5$. These optimal parameters are $\sigma = 3.7466$ Å and $\varepsilon = 0.0736$ kcal/mol, respectively.

B. Optimization methods

Global optimization of water clusters is notoriously difficult.[28,83–88] In particular, different potentials are known to produce different low-energy structures.[28,86,87] Efficient methods to sample the rugged energy landscape of water clusters include genetic algorithms[84,86] and Monte Carlo +minimization, e.g., basin hopping.[28,87] Here this method was carried out using several series of 10^4 MC moves that were further subjected to local gradient optimization. Following Wales and Hodges,[28] the MC moves involved either translational coordinates (50%) or rotational coordinates (50%) in order to improve the search for the optimal hydrogen bond network.

In addition to basin hopping, we have also carried out parallel tempering MC (Ref. 89) simulations, together with periodic quenching, to get a better confidence in the overall results. These simulations were performed with 40 replicas and a geometric progression of the replica temperatures in the range of 2–300 K. Each simulation consisted of several successive runs of 10^6 cycles per replica, and was stopped once no new global minimum was found during the last five simulations. In the propagation of the trajectories, swaps between configurations at adjacent replicas were attempted with 10% probability after each MC cycle. Configurations periodically stored from the low-temperature replicas were finally quenched to provide additional low-energy minima to the set gathered by basin-hopping optimization.

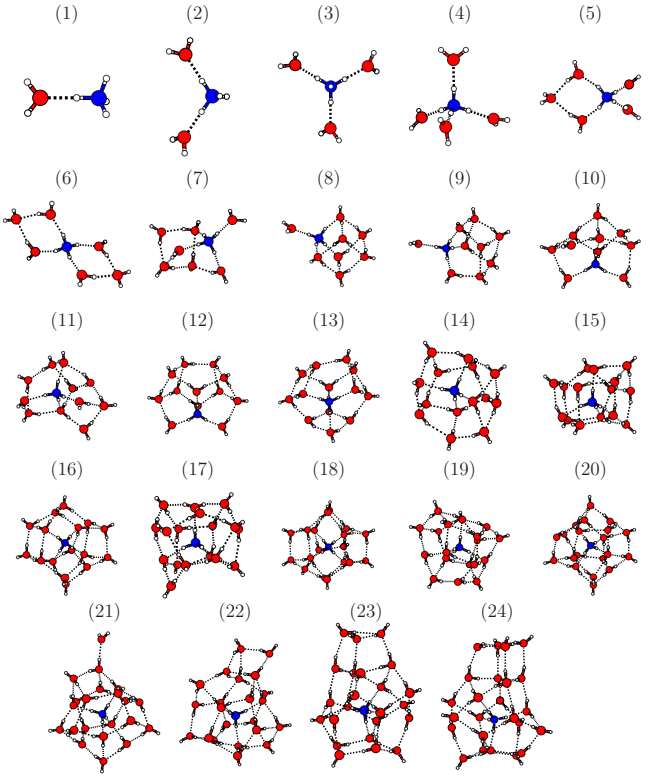

FIG. 1. (Color online) Lowest-energy structures found for $(H_2O)_nNH_4^+$ clusters using the intermolecular polarizable potential.

C. Results

The lowest-energy structures found for $(H_2O)_nNH_4^+$ $(1 \leq n \leq 24)$ using global MC optimizations are reported in Fig. 1.

The structures found in previous quantum chemical studies[34,36,43–56,66] are reproduced for clusters containing up to four water molecules. In particular, isomers other than the

global minimum appear at this size.[35,36,54,56] The structures obtained at sizes $n=5$ and 6, however, sometimes differ from those obtained from these electronic structure calculations. For $(H_2O)_5NH_4^+$, Brugé *et al.*[66] reported a global minimum with a majority of single acceptor (A) water molecules, while our most stable structure has three single acceptor/single donor (AD) molecules, in agreement with the more recent work by Lee *et al.*[55] The global minimum found by Jiang *et al.*,[54] which was based on a rhombus with two dangling water molecules, was found as a higher-lying isomer with our potential.

The most stable structure found for $(H_2O)_6NH_4^+$ only has AD water molecules, leading to two-dimensional rings or cyclic clusters linked by the ammonium impurity. It lies among the lowest isomers recently reported by Karthikeyan *et al.*[53] Single and double rings $(H_2O)_nNH_4^+$ clusters were experimentally observed by Wang *et al.*[36] in free jet expansions. From $n \geq 7$, the clusters exhibit three-dimensional geometries dominated by the double acceptor/single donor (AAD) and single acceptor/single donor motifs. Distorted cuboid structures are then found for $7 \leq n \leq 9$, with the ammonium molecule lying at a corner. A similar pattern has been theoretically found in pure[28,83,87] and protonated[15,29] water clusters. Clathratelike patterns are obtained for clusters containing more than 11 water molecules. Our results indicate that the most stable trapping site of NH_4^+ has the ion fully embedded inside a water cluster rather than being located at the surface. In particular for the magic number $n=20$, the lowest-energy structure of $(H_2O)_{20}NH_4^+$ is a 5^{12} clathrate and corresponds to a core located impurity. For this cluster, additional optimizations were carried out with the ammonium molecule at the surface. The lowest-energy structure of this kind was found to lie about 4 kcal/mol above the most stable minimum with an interior impurity (see Table II). Finally, as the cluster grows further beyond $n=20$ water molecules, a second hydration shell is progressively built while preserving the clathrate structure of the first shell. Factors influencing the relative stabilities of core/surface isomers will be discussed in more details below.

III. FIRST-PRINCIPLES CALCULATIONS

For the purpose of modeling and simplifying the sampling of the energy landscape, the empirical potential used in the previous section treated both water and ammonium as rigid molecules. We now further refine the low-energy isomers obtained with this potential using all-electron quantum mechanical methods, with no assumption about molecular flexibility or fixation of the proton on the ammonium.

A. Calculation details

The polarizable potential used in the previous section to sample the low-energy regions of the energy landscape is approximate in many respects, starting with the assumption of rigid molecules. We have locally reoptimized the stable isomers predicted by this potential using DFT. These first-principles calculations have also been carried out to determine the vibrational spectra in the infrared range, in order to compare our results with experimental measurements.[34–36,38]

All geometry and vibrational frequency calculations were carried out using the Becke3–Lee–Yang–Parr (B3LYP) hybrid functional.[90,91] We chose for the present $(H_2O)_nNH_4^+$ clusters a standard Pople-type Gaussian basis set[92–95] including polarization and diffuse functions, namely, 6-311++G(d,p). This choice was motivated by its ability to reproduce measured vibrational frequencies. Previous calculations[94–96] on NH_4^+ at the B3LYP and MP2 levels with various basis sets have shown that the smaller basis set 6-31+G(d) overestimates the experimental frequencies[97–99] by about 100 wavenumbers. Because the basis set used in this study is already quite large for use with systems containing tens of H_2O molecules, we do not expect basis set superposition errors (BSSEs) to alter the results significantly.[56] In addition, the extent of BSSE corrections needed to reach experimental agreement for ionic water complexes has been debated.[55,100,101] However, we have checked that the ordering between isomers was not affected by these errors, correcting for BSSE following the scheme of Boys and Bernardi.[102] In the so-called counterpoise procedure, the BSSE for each monomer is estimated as the difference between its energies calculated with its own basis set or with the basis of the whole complex. The total BSSE correction is then taken as the sum over all fragments. The GAUSSIAN03 series of programs were used for these DFT calculations.[103]

All minima obtained with our empirical potential remain stable upon local reoptimization using DFT. Hence the differences arising from the two approaches are essentially different orderings between isomers.

B. Results

From the total energy $E[(H_2O)_nNH_4^+]$ of the cluster and the energies $E[H_2O]$ and $E[NH_4^+]$ of the bare molecules, the formation energy is defined simply as

$$\Delta E(n) = E[(H_2O)_nNH_4^+] - E[NH_4^+] - nE[H_2O],$$

all energies being evaluated in local minimum geometries. The molecular energies $E[H_2O]$ and $E[NH_4^+]$ obtained with the 6-311++G(d,p) basis set are reported in Table I. For each cluster size n, up to ten lowest-energy minima obtained with the empirical potentials were locally reoptimized at the DFT level, and the harmonic vibrational frequencies were calculated for all resulting minima. The BSSE correction amounts to around 4 kcal/mol at size $n=5$, and about 26 kcal/mol at size $n=20$. Although significant in large clusters, these corrections do not depend too strongly on the isomer considered. In particular, no reordering between isomers was found upon including the BSSE correction in the formation energies for the cases of $(H_2O)_5NH_4^+$ and $(H_2O)_9NH_4^+$ detailed below. Hence we have omitted these corrections in Table I. However, we will include them later on in our discussion of the more sensitive case of $(H_2O)_{20}NH_4^+$.

Table I summarizes the formation energies obtained for the global minima with the empirical potential and the DFT calculations. Smaller formation energies found at the DFT level for other minima are indicated as such. This situation

TABLE I. Hydration energies (kcal/mol) of the lowest-energy structures of $(H_2O)_nNH_4^+$ clusters ($1 \leq n \leq 24$ and $n=49$). The DFT energies were calculated using the B3LYP functional and the 6-311++G(d,p) basis set, except $(H_2O)_{49}NH_4^+$, for which the smaller basis set 6-31+G(d) was used. The DFT hydration energies are given without and with the harmonic ZPE correction, and without BSSE correction. The two bottom entries are the DFT/ 6-311++G(d,p) energies of the isolated water and ammonium molecules.

n	Model	DFT	With ZPE	n	Model	DFT	With ZPE
1	−18.30	−22.01	−20.20	13	−171.84	−186.39	−150.44
2	−35.00	−40.13	−36.40	13	−171.24	−186.74	−151.45
3	−50.20	−55.50	−50.12	14	−182.90	−199.99	−161.60
4	−63.89	−68.58	−61.77	15	−195.86	−207.82	−166.38
4	−62.48	−69.72	−61.12	15	−194.70	−211.34	−170.58
5	−75.74	−82.02	−71.98	16	−208.69	−223.22	−178.33
5	−72.73	−82.67	−72.18	16	−208.25	−223.54	−178.64
6	−87.35	−95.06	−81.84	17	−220.35	−237.39	−189.97
7	−99.33	−108.74	−92.15	18	−234.29	−251.51	−200.73
7	−98.85	−109.39	−92.74	18	−234.12	−251.90	−201.02
8	−111.33	−122.29	−101.20	19	−244.83	−261.70	−208.49
8	−111.01	−121.13	−102.63	19	−244.26	−265.03	−211.98
9	−123.77	−135.23	−111.98	20	−258.29	−280.06	−223.17
9	−123.07	−136.62	−112.83	21	−267.38	−290.24	−231.45
10	−135.52	−147.51	−121.53	22	−279.02	−303.72	−241.49
10	−135.22	−148.32	−122.84	23	−290.34	−313.12	−248.41
11	−147.12	−161.70	−132.96	24	−303.91	−328.71	−259.99
12	−159.38	−173.74	−141.89				
12	−159.18	−173.99	−142.16	49	−596.78	−689.01	−540.54
H_2O		−76.46	−76.44	NH_4^+		−56.92	−56.87

actually concerns most sizes. The contribution of the zero-point energy (ZPE) correction, as obtained from DFT at the harmonic level, is also tabulated.

In absence of zero-point correction, and except for the two smallest sizes $n \leq 2$, the hydration energies obtained with the polarizable empirical potential underestimate the first-principles results. Looking at the $(H_2O)_{49}NH_4^+$ cluster (discussed below), the underestimation amounts to about 10%, not including BSSE corrections. Considering that most of the hydration energy comes from the interaction between water molecules in this large cluster, the discrepancy can probably be attributed to the parametrization of the KJ potential, rather than to the specific model used for NH_4^+.

More interestingly, the B3LYP/6-311++G(d,p) calculations lead to a frequent reordering of the isomers predicted by our potential. However, it should be noted that the DFT global minimum is also very low when calculated with the polarizable potential since it lies within about 1 kcal/mol above the empirical global minimum. Exceptions are for the $(H_2O)_5NH_4^+$ and $(H_2O)_6NH_4^+$ clusters, for which the empirical and DFT minima strongly contrast with each other. These clusters will be further discussed below.

Figure 2 shows the lowest-energy structures found for $(H_2O)_nNH_4^+$ clusters ($1 \leq n \leq 24$) using DFT that differs from the empirical global minima. The most notable changes in geometry are found for the smaller clusters $n=5$ and $n=6$, and result from the ZPE corrections. The contribution of the ZPE, which was noted earlier,[36] also affects the smaller cluster at $n=4$. Without including the ZPE, the most stable structure found for $(H_2O)_4NH_4^+$ is a rhombus in which the ammonium is only threefold hydrated. As in the case of $(H_2O)_5NH_4^+$, the changes in geometry are thus characterized by the lower coordination of the ammonium ion found at the DFT level.

The most stable structures found for $n=5$ are based on a rhombus with both methods, and do not compare with the structure reported by Brugé *et al.*[66] based on Car–Parrinello molecular dynamics, even though they agree with other DFT investigations.[34,36,54] At size $n=6$, the double ring structure found with the empirical potential is replaced by a single ring geometry with three dangling water molecules, the ammonium being still fourfold hydrated. This structural change driven by zero-point effects agrees with the recent *ab initio* study by Karthikeyan *et al.*[53]

For cluster sizes in the range $n=7-9$, the empirical and

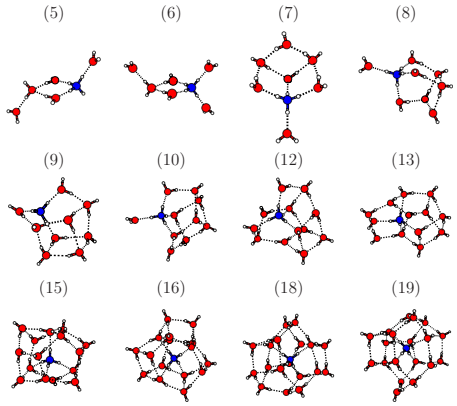

FIG. 2. (Color online) Lowest-energy structures found for $(H_2O)_nNH_4^+$ clusters at the DFT/B3LYP/6-311++G(d,p) level, after including the harmonic ZPE contribution. Only the isomers differing from the global minima found with the intermolecular potential are shown.

DFT structures differ only quantitatively but show the same pattern, the DFT structures being somewhat less compact. At sizes $n=10-13$, the DFT geometries display a marked cuboid character, whereas the empirical structures are precursors of the clathrate cage. The appearance of these precursors is slightly delayed to size $n=15$ when described from first principles. The general cage structure found for $n=15-19$ is preserved upon DFT reoptimization.

Despite these minor structural differences, the calculations involving explicit electronic structure show reasonable agreement with the results obtained using the polarizable potential. However, before attempting any comparison with experimental measurements based on spectroscopic observables, we have also quantified the possible role of temperature on the stable cluster structures.

IV. FINITE TEMPERATURE PROPERTIES

Beyond the intrinsic level of theory and modeling, the stable structures of pure or doped water clusters are also sensitive to factors such as zero-point effects, thermodynamics, and also kinetics. In this section we consider the possible role of temperature on the relative stability of different isomers of selected cluster sizes, through the simple but insightful harmonic superposition approximation.

We have also further investigated the core/surface competition in the $(H_2O)_{20}NH_4^+$ cluster, by characterizing the free energy profile related to the distance of the ammonium impurity from the cluster center of mass. For this purpose we have performed additional parallel tempering MC simulations.

A. Harmonic superposition approximation

The superposition approximation formally partitions the configuration space into its attraction basins in the energy landscape. The thermodynamical properties at equilibrium are obtained by summing over these basins.[19] This method is particularly useful for including the quantum effects of vibrational delocalization on the classical statistics obtained from sampling the energy landscape.[104,105] For a given system for which a set $\{\alpha\}$ of isomers is known, the canonical partition function at temperature T is written as

$$Z(T)=\sum_{\alpha} n_{\alpha} Z_{\alpha}(T), \tag{1}$$

in which the factor n_α accounts for the possible existence of permutation-inversion isomers. The problem consists in estimating the individual partition functions Z_α, or equivalently the isomer-specific densities of states. General methods have been proposed in the classical case,[106,107] but in the present work we limit the discussion to the simple harmonic approximation of quantum oscillators. Anharmonic corrections can be further included from the knowledge of higher order energy derivatives.[108,109] For a N-atom cluster in local minimum α, there are $3N-6$ vibrational modes with frequencies $\{\omega_{\alpha,i}, i=1\ldots 3N-6\}$ and the corresponding harmonic partition function reads

$$Z_{\alpha}(T)=\exp(-E_{\alpha}/k_BT)\prod_i \frac{\exp(-\hbar\omega_{\alpha,i}/2k_BT)}{1-\exp(-\hbar\omega_{\alpha,i}/k_BT)}, \tag{2}$$

where we have denoted E_α the energy of isomer α at its minimum. While the first exponential term on the right-hand side of Eq. (2) accounts for the internal energy of isomer α, the remaining contribution written as a product represents the entropic contribution, and also accounts for the zero-point correction in the numerator. From the set of frequencies $\{\omega_{\alpha,i}\}$, energies $\{E_\alpha\}$, and purely geometrical factors $\{n_\alpha\}$, the equilibrium probability that the cluster lies in isomer α is $p_\alpha=n_\alpha Z_\alpha/Z$.

We have applied the harmonic superposition method to two selected $(H_2O)_nNH_4^+$ clusters with $n=5$ and $n=9$, respectively. For each cluster, the energies and frequencies of all isomers have been obtained using the same explicit treatment of electronic structure as described in Sec. III, that is DFT/B3LYP with the 6-311++G(d,p) basis set.

The ten lowest-energy isomers obtained for the smaller cluster $(H_2O)_5NH_4^+$ are represented in Fig. 3 and sorted according to their hydration energies. Their ordering with the polarizable potential, also indicated on this figure, is quite different from the DFT ordering. However, all isomers lie within about 2.6 kcal/mol of each other. The three lowest-energy isomers are very close to each other, which somewhat mitigates that the empirical global minimum is only the third lowest DFT minimum. The two most stable structures are closely related to each other, and differ by the location of the single acceptor water molecule bound to another water molecule. As was discussed in Sec. III, structures with a four-hydrated ammonium ion are not the most stable isomers. In particular, the structure considered by Brugé *et al.*[66] lies only at fourth rank (second rank with the polarizable potential). However, the variety of structures shown in Fig. 3 is more similar to those reported by Jiang *et al.*[54]

The effects of temperature are illustrated on the canonical probabilities of visiting the four lowest DFT isomers, as represented in the bottom of Fig. 3. The probabilities of visiting the six remaining isomers never exceed a few percents, even at 300 K, and they have been omitted from this graph.

In the $(H_2O)_5NH_4^+$ cluster, the two lowest-energy isomers are found in comparable proportions at about 30 K, and these isomers dominate up to 250 K, above which the fourth isomer becomes competitive. The poor contribution of the third isomer, while energetically stable, is due to its lower entropy related to higher vibrational modes. Conversely, isomers 1, 2, and 4 have rather floppy modes of the single acceptor water molecule. The present calculation indicates that, under normal experimental conditions, the $(H_2O)_5NH_4^+$ cluster mainly consists of its two first rhombus-based isomers in the approximate 65%/35% ratio, the other structures being negligibly populated. This mixing will have important consequences on the spectroscopic observables.

Before turning to our second example of $(H_2O)_9NH_4^+$, the cluster at $n=5$ was further considered in order to quantify the cost of moving the proton of the ammonium onto a water molecule. Early Hartree–Fock quantum chemical calculations[49] suggested that the proton would be completely transferred to a water molecule in both $(H_2O)_3(NH_3)H^+$ and

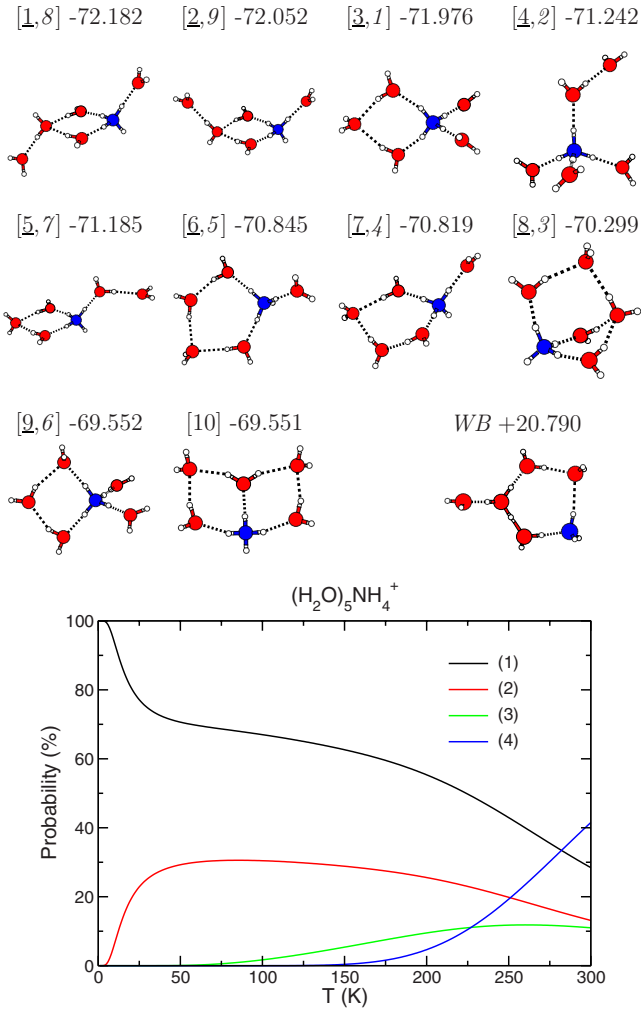

FIG. 3. (Color online) The ten lowest-energy isomers of $(H_2O)_5NH_4^+$. The isomers are ordered according to their DFT energy (underlined numbers), and their ordering in the polarizable model is given in italics. The formation energies are indicated in kcal/mol. The structure labeled WB has the extra proton localized on water molecules through the formation of an Eigen complex. The bottom panel shows the equilibrium probabilities of visiting the four lowest-energy isomers obtained with the harmonic superposition approximation as a function of temperature.

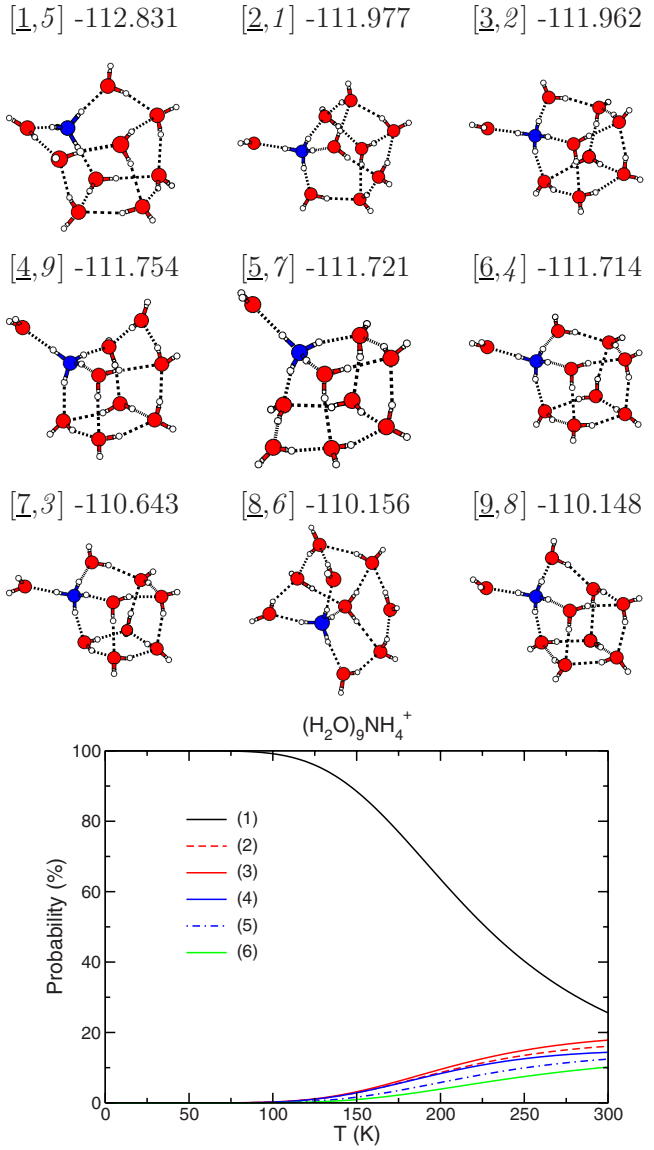

FIG. 4. (Color online) The nine lowest-energy isomers of $(H_2O)_9NH_4^+$. The isomers are ordered according to their DFT energy (underlined numbers), and their ordering in the polarizable model is given in italics. The formation energies are indicated in kcal/mol. The bottom panel shows the equilibrium probabilities of visiting the six lowest-energy isomers obtained with the harmonic superposition approximation as a function of temperature.

$(H_2O)_4(NH_3)H^+$. Most of our attempts to stabilize the proton on a water molecule at the B3LYP/6-311++G(d,p) level were unsuccessful due to the spontaneous migration of the proton back to the ammonia along successive formations of hydronium ions. One stable conformation could eventually be obtained with a stable Eigen complex, as shown in Fig. 3, separated from other ammonium-bound structures. However, its energy is much higher than the global minimum by about 93 kcal/mol. Thus we do not expect conformations with the proton localized on a water molecule to be significantly populated at such small cluster sizes. This matches the conclusions of the dynamical study by Cheng,[41] in which the proton was found to naturally transfer from hydronium to ammonia in small $(H_2O)_nNH_4^+$ clusters.

The nine lowest-energy isomers found for the $(H_2O)_9NH_4^+$ cluster are shown in Fig. 4, along with their ordering with the polarizable model. These isomers generally share a common structural pattern consisting of a square facing a pentagon and one dangling water molecule. The global DFT minimum geometry does not have this single acceptor water molecule, and contrary to most other isomers the ammonium impurity is only threefold hydrogen bonded to the cluster. Its energetic stability is quite substantial (near 0.9 kcal/mol), whereas the five next isomers lie in a restricted energy range (0.3 kcal/mol).

The variations with temperature of the probabilities of visiting the six lowest-energy isomers are also displayed in Fig. 4. In agreement with its energetic stability, the global minimum is the most stable up to 300 K. The five next isomers contribute with comparable amounts, and compete significantly with the global minimum above 200 K. While the smaller $(H_2O)_5NH_4^+$ cluster essentially exhibits simple isomerization, the higher-lying isomers of $(H_2O)_9NH_4^+$ cannot be neglected at this temperature.

B. Monte Carlo simulations

The cluster $(H_2O)_{20}NH_4^+$ has far too many isomers to attempt a harmonic superposition approach based on DFT properties. The most stable surface-impurity minimum, which lies about 4 kcal/mol above the core-impurity minimum, remains the least stable of these two isomers after reoptimizing with DFT (see also a more detailed discussion below in Sec. V B). However, temperature effects may directly influence the favored location of the impurity, especially near the melting phase change. Using MC simulations, we have investigated the thermal stability of the ammonium impurity in the cluster as a function of temperature.

The energy landscape of the $(H_2O)_{20}NH_4^+$ cluster is expected to be as rough as that of the pure 20-molecule water cluster.[19] Analyzing the results of our parallel tempering MC simulations, we could not find evidence for a possible structural transition involving the ammonium impurity going from the core to the surface of this cluster. Nevertheless, when initiated from the lowest isomers with the impurity in the core or at the surface, these simulations provide independent estimates of the cluster melting point, defined here as the temperature at which the impurity becomes thermally delocalized inside the entire cluster volume. The simulations consisted here of 40 replicas with temperatures distributed following two regular progressions in the ranges 5–100 and 100–300 K by steps of 5 and 10 K, respectively. For each trajectory (10^8 MC steps and 10^7 extra equilibration steps) the distance d of the nitrogen atom to the cluster center of mass was monitored.

From the simulation initiated at the global minimum geometry (with a core NH_4^+ impurity), the two-dimensional histograms $p(d,E)$ of distance d and potential energy E were recorded for further reweighting analysis.[110] Here we assume that in the vicinity of the melting point, both the core and surface states of the cluster will be partly sampled by our simulations, while such a sampling would be much more difficult at low temperatures.

After reweighting, the histograms $p(d,E)$ are transformed into temperature-dependent probabilities $p(d,T)$ of finding the NH_4^+ impurity at distance d from the center of mass. This quantity is best discussed in terms of the potential of mean force, defined as a Landau free energy according to

$$F(d,T) = -k_B T \ln p(d,T).$$

The variations of F with d are shown in Fig. 5 at the three temperatures $T=150$, 190, and 230 K. We have also represented in Fig. 5 the thermal average $\langle d\rangle(T)$ for clusters having the ammonium impurity in the core or at the surface at the beginning of the simulation.

The average distance $\langle d\rangle$ smoothly increases (core impurity cluster) or decreases (surface impurity cluster) until both values merge to $\langle d\rangle \simeq 1.9$ Å near $T \simeq 210$ K. The sharp variations exhibited by $\langle d\rangle$ occur at about 190 K, which gives us an estimate of the melting range, in agreement with other thermodynamical indicators such as the internal energy (results not shown).

The free energy profile $F(d,T)$ at 150 K shows two main basins near the core ($d \sim 0.2$ Å) and near the surface ($d \sim 3.6$–4.1 Å). The free energy difference between these basins is comparable to the energy difference (about 4 kcal/mol) between the two isomers. The barrier between the basins is not significantly higher, and barely exceeds 5 kcal/mol at this temperature. At the melting point, the surface isomers are only 2 kcal/mol less stable in free energy than the core isomers. More importantly, the impurity can now be partly stabilized in intermediate regions of the cluster, as seen from the shallow basin near $d \sim 2.5$ Å. The free energy barrier is strongly reduced below 2.5 kcal/mol. Finally, at 230 K, the free energy only shows a single very broad minimum corresponding to the melted state.

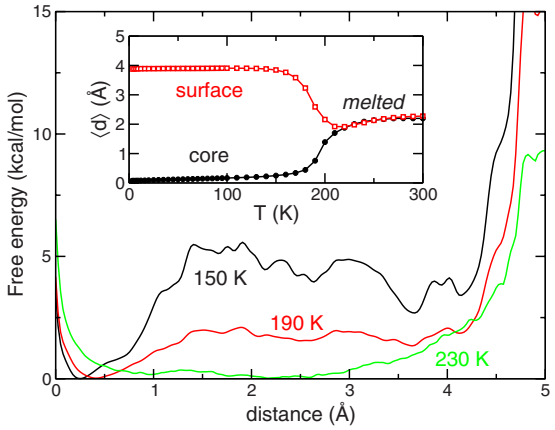

FIG. 5. (Color online) Landau free energy as a function of the distance d of the NH_4^+ impurity inside the $(H_2O)_{20}$ cluster, obtained with the polarizable model and MC simulations at three temperatures. The inset shows the average value $\langle d\rangle$ obtained from MC simulations, initiated from structures with the impurity in the core or at the surface.

The barrier of $E^\dagger \simeq 2.5$ kcal/mol for core/surface isomerization is rather moderate, making it easy to cross at 190 K. A simple transition state theory estimate of the crossing rate $k \sim \nu_0 \exp(-E^\dagger/k_B T)$, with $\nu_0 \sim 1$ ps^{-1} a typical attempt frequency, gives $k_0 \simeq 10^{-4}$ ps^{-1} at 190 K. These results show that temperature effects enhance the chances that the ammonium impurity is located on the surface of the water cluster. Purely entropic effects play an additional but similar role, the number of surface sites being larger than in core isomers. Combined together, these two effects may be sufficient to explain the favored surface location of NH_4^+ in water clusters suggested by recent experiments.[38,39]

V. SPECTROSCOPIC SIGNATURES

We mainly focus our spectral study on the O–H stretching vibrational region (3600–3800 cm^{-1}) in order to carry out a detailed structural analysis of clusters $(H_2O)_nNH_4^+$ with $5 \le n \le 21$. To facilitate comparison with experiments,[34–36,38] the calculated harmonic frequencies have been scaled by a constant factor f and broadened using Lorentzian linewidths of ten wavenumbers. The scaling factor results from the lack of static electron correlation effects in DFT, and approximately corrects for the tendency of single-determinant wave functions to overestimate bond dissociation energies. The linewidth roughly matches the experimental broadenings in the free O–H stretch bands.

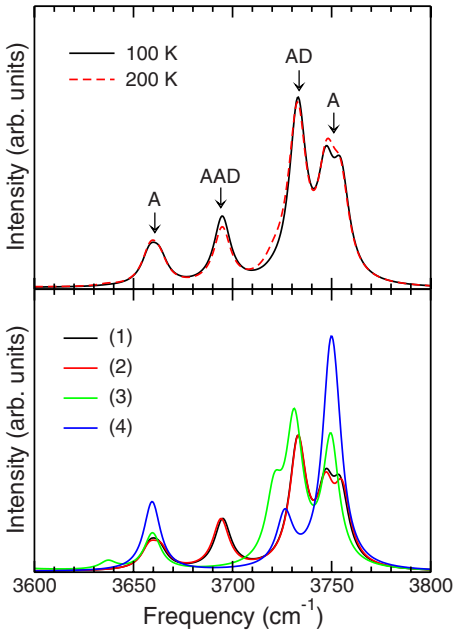

FIG. 6. (Color online) Calculated vibrational spectra of $(H_2O)_5NH_4^+$ in the 3600–3800 cm^{-1} range. A 10 cm^{-1} broadening is used for each frequency. Upper panel: Spectrum averaged over all isomers at 100 and 200 K. The four main O–H stretching bands are assigned a type A, AD, or AAD, according to the nature of the O–H vibration (see text for details). Lower panel: Isomer-resolved spectrum for the four lowest-energy structures.

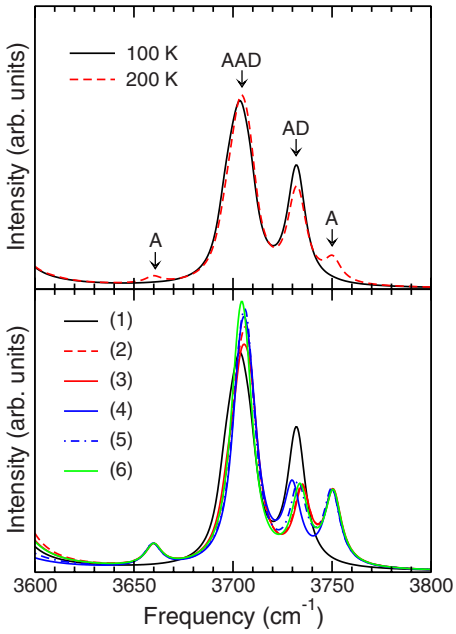

FIG. 7. (Color online) Calculated vibrational spectra of $(H_2O)_9NH_4^+$ in the 3600–3800 cm^{-1} range. A 10 cm^{-1} broadening is used for each frequency. Upper panel: Spectrum averaged over all isomers at 100 and 200 K. The four main O–H stretching bands are assigned a type A, AD, or AAD, according to the nature of the O–H vibration (see text for details). Lower panel: Isomer-resolved spectrum for the six lowest-energy structures.

The empirical scaling factor f depends on both the functional and the basis set. For the present DFT calculations using the B3LYP functional and the 6-311++G(d,p) basis set, the optimum value was taken as $f=0.9604$, as recommended by various authors,[111,112] based on benchmark calculations on many molecules. The density-functional calculations provided the positions of the vibrational lines and the intensities at maximum.

As will be seen below, our calculations of the vibrational spectra lead to conclusions similar to those obtained from previous studies[12,13] on protonated water clusters $(H_2O)_nH^+$. In particular, the O–H stretching region splits into a multiplet of bands at small cluster sizes $(n \leq 8)$, simplifying into a doublet at intermediate sizes $(9 \leq n \leq 19)$, and eventually merging into a single band as n reaches the magic size 20.

A. $(H_2O)_5NH_4^+$ and $(H_2O)_9NH_4^+$

We first consider the infrared spectra of small clusters, for which the equilibrium state is described using the harmonic superposition approximation detailed in Sec. IV A. From this approach, the statistical weights of the various isomers are estimated using their static properties, namely, energies and vibrational frequencies. The linewidth of 10 cm^{-1} being a fixed parameter in our calculations, we do not account for additional temperature broadening effects.

Figure 6 shows the infrared spectra calculated for the cluster $(H_2O)_5NH_4^+$ at the two temperatures $T=100$ K and 200 K, as well as the individual contributions of the four lowest-energy isomers.

Four distinct free O–H band locations, labeled A, AAD, AD, and A on the figure, are found for this cluster. The two outer A bands correspond to the symmetric (3660 cm^{-1}) and asymmetric (3750 cm^{-1}) stretching vibrations of a water molecule in a single acceptor configuration. The strong intensity of these modes suggests open or cyclic structures, in agreement with the configurations shown in Fig. 3. The two intermediate bands near 3695 and 3730 cm^{-1} are associated with the stretching vibrations of water molecules in double acceptor/single donor and single acceptor/single donor configurations, respectively. The frequencies of these four bands do not vary appreciably with cluster size, however their relative intensities exhibit clear variations.

Figure 7 shows the vibrational spectra of $(H_2O)_9NH_4^+$ calculated at the same two temperatures of 100 and 200 K, as well as the decomposition into the contributions of the six lowest-energy isomers. At 100 K, only two distinct free O–H bands corresponding to AAD and AD configurations are clearly identified in this part of the infrared spectrum. The corresponding frequencies of these two modes are closer to those calculated for the smaller cluster. The most intense band is found for the O–H stretching of the AAD water molecules. This is directly related to the stable geometry of this cluster (see Fig. 7), which is dominated by AAD molecules. However, upon increasing the temperature, a small contribution of the symmetric and antisymmetric O–H stretching vibrations labeled A in Fig. 7 is found at 200 K. These modes are clearly associated with the emergence of isomers other than the global minimum at this temperature (see Fig. 4) even though the global minimum remains the most abundant isomer. Consistently with the calculated spectrum, these five isomers have in common a single acceptor water molecule.

The infrared spectrum near the O–H stretching bands was also calculated for the lowest-energy minima of larger $(H_2O)_nNH_4^+$ clusters with $10 \leq n \leq 19$. The results (not

TABLE II. Formation energies (in kcal/mol) of the two lowest-energy isomers of $(H_2O)_{20}NH_4^+$ found with the impurity either in the core or at the surface of the cluster. The DFT calculations have been performed with two basis sets, and possibly completed with ZPE and BSSE (on top of ZPE) corrections. Additional single-point RIMP2 energy calculations using second-order perturbation theory with the 6-311++G(d,p) and aug-cc-pVDZ basis sets are also reported, with additional BSSE corrections (not including ZPE).

Location of impurity	Method of calculation	Basis set	Hydration energy (kcal/mol)	With ZPE (kcal/mol)	With BSSE (kcal/mol)
Core	Potential		−258.29		
Surface	Potential		−254.51		
Core	DFT/B3LYP	6-31+G(d)	−302.24	−242.41	−202.81
Surface	DFT/B3LYP	6-31+G(d)	−300.88	−240.64	−200.85
Core	DFT/B3LYP	6-311++G(d,p)	−280.06	−223.17	−196.75
Surface	DFT/B3LYP	6-311++G(d,p)	−278.05	−220.96	−194.61
Core	RIMP2	6-311++G(d,p)	−296.45		−230.94
Surface	RIMP2	6-311++G(d,p)	−293.51		−228.56
Core	RIMP2	aug-cc-pVDZ	−362.48		−320.53
Surface	RIMP2	aug-cc-pVDZ	−361.22		−320.28

shown) are essentially similar to those reported in Fig. 7 for $(H_2O)_9NH_4^+$, and display two main bands corresponding to the AAD and AD motifs.

The present results agree with the experimental measurements by Wang and co-workers[34–36] and by Diken *et al.*:[38] The four A, AD, and AAD bands found for $n=5$ evolve into only two intense AAD and AD bands for clusters containing $n=9$ water molecules or more.

B. The core/surface dilemma: $(H_2O)_{20}NH_4^+$ and neighboring sizes

We now return to the case of the magic number $n=20$, for which we have carried out similar spectroscopic calculations. However, our aim here is to compare the spectral signatures of the two most stable isomers having the ammonium impurity either in the core or at the surface of the $(H_2O)_{20}NH_4^+$ cluster, as provided by our global optimizations with the empirical potential.

Considering the special status of this cluster, the DFT minimizations were repeated using the B3LYP hybrid functional with different basis sets, namely, 6-31+G(d) and 6-311++G(d,p). Additional single-point calculations were carried out using perturbation theory [RIMP2 (Refs. 113 and 114)] with both 6-311++G(d,p) and aug-cc-pVDZ (Refs. 115 and 116) basis sets, including BSSE corrections.

The most stable trapping site of NH_4^+ in the water cluster is identified by the hydration energy ΔE, possibly including the zero-point correction in the case of the DFT minimizations. The formation energies obtained at the various levels of theory are listed in Table II for the surface and core isomers. For an easier comparison, the hydration energies obtained with the empirical potential are also given.

The most stable conformation of $(H_2O)_{20}NH_4^+$ is found with the ammonium ion in the core of the clathrate cage at all levels of theory, irrespective of the inclusion or neglect of ZPE and BSSE corrections. The energy difference between the two isomers lies in the range of 1–4 kcal/mol depending on the calculation level. These values are comparable to the barrier for core/surface isomerization estimated in Sec. IV B, hence the surface structure could well be preferred over the core structure simply due to entropic effects. The greater energetic stability of the core isomer is at variance with the results of other DFT calculations.[38,39] They are in better agreement with the *ab initio* results obtained by Khan,[57] who found that the core and surface isomers of $(H_2O)_{20}NH_4^+$ were nearly degenerate. However, it should be noted that the surface isomer considered by this author has its four H atoms contributing to the hydrogen bond network, in contrast with the lowest surface configurations found in both the present work and in the study by Diken *et al.*[38] This makes a full comparison with Khan's results somewhat less relevant. We finally note that the lowest structure found by Diken and co-workers is actually slightly lower in energy than our best surface structure (when calculated at the DFT+ZPE level), however it is not more stable than our core global minimum.[117]

A possible discrimination between core and surface isomers was suggested by Diken *et al.*[38] based on differences in the mid-IR spectra. We have represented in Fig. 8 the vibrational spectrum calculated in the broad range 0–4000 cm^{-1}, for both core and surface isomers of $(H_2O)_{20}NH_4^+$, but also for the most stable structures obtained at sizes $n=19$ and 21. The geometries found for these clusters correspond to a fully solvated ammonium impurity.

The O–H stretching bands in the 3600–3800 cm^{-1} domain are highlighted in the bottom panel of Fig. 8. According to our DFT calculations, the AAD/AD doublet previously found in the O–H stretching region persists throughout the size range $9 \leq n \leq 19$. However, the AD band is no longer seen for clusters having 20 or more water molecules, irrespective of the impurity location in the cluster. Strikingly, the spectra obtained for the core and surface isomers of $(H_2O)_{20}NH_4^+$ are very similar, and do not show any specific signature. These results only partially agree with the other DFT calculations by Diken *et al.*[38] We likewise find that the core isomer of $(H_2O)_{19}NH_4^+$ has a clear AD band, while the surface isomers of $(H_2O)_{20}NH_4^+$ and $(H_2O)_{21}NH_4^+$ do not. However, the core isomer of the same cluster, which is found at the present level of calculation to be more stable than the surface isomer, also does not have such a spectroscopic sig-

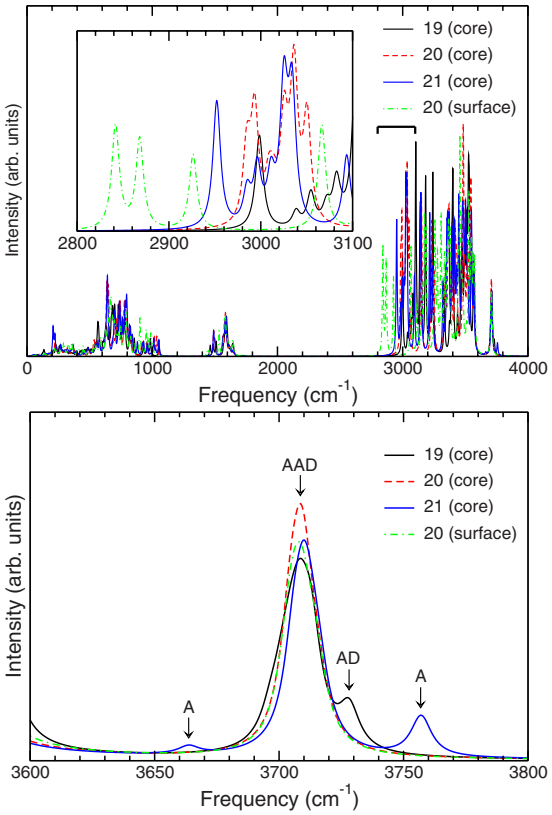

FIG. 8. (Color online) Calculated vibrational spectra of $(H_2O)_nNH_4^+$ clusters, $n=19-21$. For $n=20$, the ammonium impurity can be located in the core or at the surface. The upper panel shows the entire spectra in the range of 0–4000 wavenumbers. The inset highlights the N–H stretching region near 2800–3100 cm^{-1}. The lower panel emphasizes the O–H stretching bands near 3600–3800 cm^{-1}, with the same labeling as in Figs. 6 and 7.

nature. A possible explanation for the difference with the DFT results of Diken *et al.*[38] might come from the different structure of the core species considered by these authors. Even then, our results suggest, as in the case of pure water clusters, that the infrared signature associated with O–H stretching does not provide sufficient evidence for a complete structural characterization of $(H_2O)_nNH_4^+$ clusters.

Despite this rather deceptive result, we have further analyzed the vibrational spectra near the N–H stretching bands. A geometric signature could be anticipated here due to the dangling N–H bond in surface structures, whereas the ammonium is fourfold hydrated when in the core. Unfortunately, the free N–H band is found near 3340 cm^{-1} at the present level of calculation, which falls right into a background of strong O–H stretching transitions. Nevertheless, interesting differences are seen in the 2800–3100 cm^{-1} domain, highlighted in the inset in the upper panel of Fig. 8. In this figure the difference between core and surface isomers is striking, transitions being found near 2800–2900 cm^{-1} only in the latter case. These bands are related to the existence of a dangling N–H bond in the surface isomer, whereas the ammonium molecule is fourfold hydrogen bonded in the other core isomers. These results might open a more sensitive way toward structural characterization of fully hydrated $(H_2O)_nNH_4^+$ clusters.

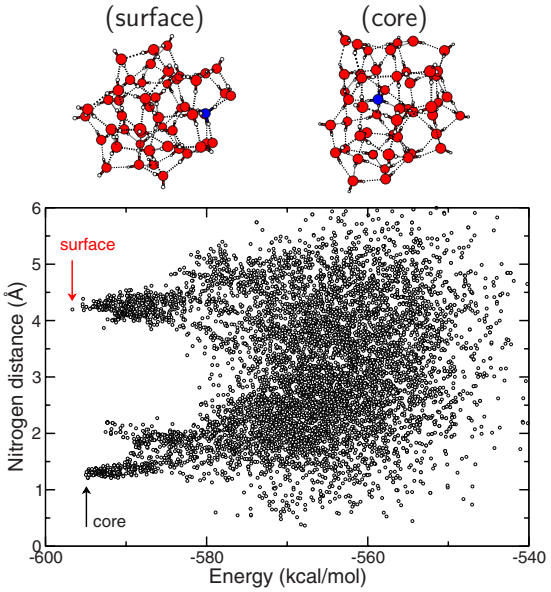

FIG. 9. (Color online) Distance from the nitrogen atom to the cluster center of mass against the energy minimum, as obtained from MC optimizations of the $(H_2O)_{49}NH_4^+$ cluster. The vertical arrows locate the lowest-energy minima for each category, as represented on the top panel.

VI. EXAMPLE OF A LARGER CLUSTER

It takes a significant number of molecules for a water cluster to exhibit crystalline features.[85] Using the TIP4P potential and the more sophisticated TTM2 rigid model, Kazimirski and Buch[85] found that clusters containing up to 293 water molecules lie below this crystalline crossover size, showing an amorphous character, only the largest cluster showing some crystalline core. These conclusions have been revised by Bandow and Hartke,[88] who found based on the flexible version of the TTM2 that relaxed ice structures were competitive already above 90 molecules. In any case, the dodecahedral structures obtained previously for cluster sizes below $n=21$ are clearly far below this crystalline crossover.

As an attempt to investigate the structural preferences of the ammonium impurity in larger water clusters, global optimization MC simulations have been performed for the $(H_2O)_{49}NH_4^+$ cluster using both basin hopping (10^5 local optimizations) and parallel tempering (ten sets of 10^6 MC cycles per replica followed by systematic quenching). Considering the huge number of stable minima on the energy landscape of this cluster, we cannot be confident that our very limited searches have produced the actual global minimum. However, because we initiated our searches from structures with the impurity located in the core or at the surface, we believe that our survey has been complete enough to distinguish low-energy isomers belonging to these important classes.

The most stable surface and core structures found for the $(H_2O)_{49}NH_4^+$ cluster are represented in Fig. 9. This figure also displays the correlation between the isomer energy and the distance d of the nitrogen atom for all structures obtained from the MC optimizations. This plot clearly shows the existence of two series of low-lying isomers with energy below −585 kcal/mol corresponding to the ammonium either near the core ($d\sim1.2$ Å) or at the surface ($d\sim4.2$ Å). Minima

among each of these branches mainly differ in their hydrogen bond network. The global minimum is found at −596.78 kcal/mol with the ammonium located at the surface. The lowest-energy minimum with the ammonium in the core is only at −594.99 kcal/mol. Both minima are three-dimensional compact structures containing square, pentagonal, and hexagonal outer faces that are also found in pure water clusters.[85] Noteworthy, the NH_4^+ impurity is fourfold coordinated in these two structures.

Even though the success of global optimization can be questioned for such clusters, the present findings show that surface and core structures tend to become energetically similar as size increases. The surface impurity found for this species could thus reconcile our results with the conclusions reached by previous theoretical investigations about the preferred location of ammonium in water clusters.[38,39]

The most stable isomers of $(H_2O)_{49}NH_4^+$ were further reoptimized using DFT with the B3LYP hybrid functional. For this rather large system, the basis set was restricted to the smaller 6-31+G(d) set in order to reach convergence in the electronic structure within reasonable computer time. Upon local optimization, the surface isomer has a formation energy of about −689.01 kcal/mol, significantly lower than the core isomer (−686.79 kcal/mol). This energy difference slightly decreases after including the zero-point vibrational energy (−540.54 kcal/mol versus −539.07 kcal/mol for the surface and core isomers, respectively).

The infrared spectra were also computed with 10 cm^{-1} linewidth, but with the scaling factor $f=0.9735$ previously used in Ref. 38 at this same level of theory. The spectra for the two structures are quantitatively similar in the range of 2800–2900 cm^{-1} and near 3700 wavenumbers (results not shown). In particular, a single AAD band dominates the spectrum in the O–H stretching region. Concerning N–H stretching, no frequency is found in the 2800–2900 cm^{-1} range, consistently with the ammonium impurity being fourfold hydrogen bonded in this large cluster.

VII. SUMMARY AND CONCLUSION

One of our ultimate goals is to determine the thermal properties of charged water clusters and to characterize their resistance to evaporation. These species consist either of pure but protonated water clusters, or water molecules doped with a charged impurity. The latter case, with the ammonium molecule as the impurity, was investigated first for the relatively simpler modeling of its intermolecular interactions. Contrary to protonated water clusters, the proton in ammonium-water clusters essentially localizes on the ammonium ion, making explicit empirical potentials usable for this problem.

In the present work, we have investigated the stable structures of $(H_2O)_nNH_4^+$ clusters using a variety of theoretical methods. Global optimization of candidate structures was first performed using a polarizable potential adapted from the KJ water potential[70,71] and from the Dang model for ammonium.[65] Global optimization was carried out using MC sampling with local minimizations. The stable structures were subsequently reoptimized using DFT with the B3LYP hybrid functional and the relatively large 6-311++G(d,p) basis set. ZPE corrections obtained from these DFT calculations were also considered, at the harmonic level. Using the superposition approximation, the relative stability of various isomers at finite temperature was also quantified.

The global minima found for $(H_2O)_nNH_4^+$ are generally similar to the stable structures known for pure protonated water clusters, and consist of arrangements of square and pentagonal faces forming irregular cuboids, and evolving into clathratelike cages as the number of molecules reaches the dozen. A dodecahedral cage is obtained at size $n=20$, with clear precursors already seen at $n=15$. Our calculations suggest that the NH_4^+ molecule is energetically more stable when fully hydrated at the center of the cluster. In particular, dedicated optimizations of stable structures for the magic number $n=20$ with the impurity either at the core or at the surface confirm that the core isomer is more stable by a few kcal/mol. However, at size $n=49$ the ammonium molecule preferably binds near the surface of our putative global minimum, even though the most stable core isomer is less than 2 kcal/mol lower in energy.

For many sizes, some reordering between isomers occurs after reoptimizing them using DFT, starting from empirical potential geometries. However, the empirical and DFT global minima are generally close in energy, indicating that our potential is not too unrealistic. The contribution of the ZPE may induce some reorderings, particularly at the small sizes $n=4-6$. In agreement with previous quantum chemical calculations,[36,49,53–56] several isomers with noticeably different geometries lie within less than one kcal/mol from each other.

Due to this competition, temperature effects are found to influence cluster structure significantly at small sizes. The $(H_2O)_5NH_4^+$ cluster, in particular, has two related isomers based on the same rhombus pattern, which remain stable up to about 200 K. The global minimum of $(H_2O)_9NH_4^+$, on the other hand, stays the most stable isomer up to 200 K. This temperature is also found as the melting temperature of the larger $(H_2O)_{20}NH_4^+$ cluster, as inferred from additional MC simulations.

In order to compare with available measurements,[34–36,38] the vibrational spectra were computed in the infrared range using DFT with appropriate frequency scaling factors and a fixed broadening of ten wavenumbers. Our results agree well with experimental data, and also with theoretical calculations (most often at the DFT level).[36,38,54] In particular, in the O–H stretching region of 3600–3800 cm^{-1}, the four bands corresponding to single acceptor, single acceptor/single donor, and double acceptor/single donor motifs are seen to evolve for $5 \leq n \leq 19$ into two main AAD and AD bands, before eventually the AAD band dominates. Relating now these bands to the location of the ammonium impurity in the cluster, two different isomers were found to have common spectroscopic identities in the 3600–3800 cm^{-1} range. This questions the conclusions reached by Diken *et al.*[38] about the location of NH_4^+ in the water cluster on O–H stretching frequencies. However, looking at the 2800–3100 cm^{-1} range, the presence of dangling N–H bonds of a surface impurity was clearly identified, suggesting an alternative experimental

probe. One possible source for the discrepancy between our results and the conclusions reached by Diken *et al.*[38] could lie in that the experiments performed by these authors may not sample an equilibrium distribution of isomers.

Among the results obtained in this work, the most salient one is probably the very similar binding energies of the surface and interior sites of the ammonium molecule in medium-size water clusters. This conclusion somewhat contrasts with some calculations of other groups.[38,39] The competition between isomers is primarily driven by the differences in water-water and water-ammonium interactions. However, as in protonated water clusters, the outer or inner location of the impurity readily affects the overall energetic stability via different polarization contributions. This competition is already apparent in small clusters such as $(H_2O)_4NH_4^+$ or $(H_2O)_5NH_4^+$. Our selection of structures strongly relies on the global optimization results based on an empirical potential, even though we tried to remove some of this bias by reoptimizing structures with a surface impurity but a higher energy. For the water-ammonium part, the empirical potential was partly fitted to reproduce the detailed DFT results obtained by Brugé *et al.*[66] However, as shown by previous groups[36,54,55] and by our own B3LYP/6-311++G(d,p) calculations, the stable structure reported by these authors for $(H_2O)_5NH_4^+$ is far from being the lowest, and even lacks an extra hydrogen bond. However, before fitting again the parameters of the ammonium interaction, it would be useful to ascertain the electronic structure benchmark calculations on those small clusters using alternative quantum chemistry methods. Besides, the water-water part was taken without modification from KJ (Refs. 70 and 71) and should perhaps be revised.

Beyond structural properties, a natural extension of this work would be to characterize the evaporation dynamics of water-ammonium clusters, in relation with nucleation phenomena. Several theoretical approaches are available to study unimolecular dissociation, including dynamical nucleation theory[118] and phase space theory.[119] Both approaches are statistical and based on ideas from transition state theory. Their application heavily requires ingredients such as free energies or densities of states, which can all be computed using appropriate simulation techniques, provided that the potential energy surface can be prone to efficient sampling. This emphasizes the need for accurate intermolecular potentials.

ACKNOWLEDGMENTS

This work was funded by the ANR grant NUCLEA. We thank J.-M. L'Hermite, S. Zamith, F. Chirot, and P. Labastie for fruitful discussions. The calculations were partially carried out at the CALMIP computer center, which we gratefully acknowledge. We also thank M. Schmidt and K. D. Jordan for useful correspondence.

[1] R. G. Keesee, J. Geophys. Res. **94**, 14683 (1989).
[2] R. P. Wayne, *Chemistry of Atmospheres*, 3rd ed. (Oxford University Press, Oxford, 2000).
[3] G. Nidener-Shatteburg and V. E. Bondybey, Chem. Rev. (Washington, D.C.) **100**, 4059 (2000).
[4] J. J. Gilligan, D. J. Moody, and A. W. Castleman, Jr., Z. Phys. Chem. **214**, 1383 (2000).
[5] H. G. Kjaergaard, T. W. Robinson, D. L. Howard, J. S. Daniel, J. E. Headrick, and V. Vaida, J. Phys. Chem. A **107**, 10680 (2003).
[6] P. G. Sennikov, S. K. Ignatov, and O. Schrems, ChemPhysChem **6**, 392 (2005).
[7] W. W. Duley, Astrophys. J. **471**, L57 (1996).
[8] L. A. Lipscomb, M. E. Peek, F. X. Zhou, J. A. Bertrand, D. VanDerveer, and L. D. Williams, Biochemistry **33**, 3649 (1994).
[9] S. S. Lin, Rev. Sci. Instrum. **44**, 516 (1973).
[10] J. Q. Searcy and J. B. Fenn, J. Chem. Phys. **77**, 2549 (1974).
[11] S. Wei, Z. Shi, and A. W. Castleman, J. Chem. Phys. **94**, 3268 (1991).
[12] M. Miyazaki, A. Fujii, T. Ebata, and N. Mikami, Science **304**, 1134 (2004).
[13] J.-W. Shin, N. I. Hammer, E. G. Diken, M. A. Jonson, R. S. Walters, T. D. Jaeger, M. A. Duncan, R. A. Christie, and K. D. Jordan, Science **304**, 1137 (2004).
[14] C.-C. Wu, C.-K. Lin, H.-C. Chang, J.-C. Jiang, J.-L. Kuo, and M. L. Klein, J. Chem. Phys. **122**, 074315 (2005).
[15] T. James and D. J. Wales, J. Chem. Phys. **122**, 134306 (2005).
[16] S. S. Iyengar, M. K. Petersen, T. J. F. Day, C. J. Burnham, V. E. Teige, and G. A. Voth, J. Chem. Phys. **123**, 084309 (2005).
[17] K. I. Suhara, A. Fujii, K. Mizuse, N. Mikami, and J.-L. Kuo, J. Chem. Phys. **126**, 194306 (2007).
[18] H. Yu and Q. Cui, J. Chem. Phys. **126**, 213101 (2007).
[19] D. J. Wales, *Energy Landscapes* (Cambridge University Press, Cambridge, England, 2003).
[20] K. Laasonen and M. L. Klein, J. Phys. Chem. **98**, 10079 (1994).
[21] A. Khan, Chem. Phys. Lett. **217**, 443 (1994).
[22] A. Khan, Chem. Phys. Lett. **319**, 440 (2000).
[23] C. V. Ciobanu, L. Ojamäe, I. Shavitt, and S. J. Singer, J. Chem. Phys. **113**, 5321 (2000).
[24] R. A. Christie and K. D. Jordan, J. Phys. Chem. A **105**, 7551 (2001).
[25] D. J. Wales and I. Ohmine, J. Chem. Phys. **98**, 7245 (1993).
[26] C. Tsoo and C. L. Brooks III, J. Chem. Phys. **101**, 6405 (1994).
[27] J. A. Niesse and H. R. Mayne, J. Comput. Chem. **18**, 1233 (1997).
[28] D. J. Wales and M. P. Hodges, Chem. Phys. Lett. **286**, 65 (1998).
[29] M. P. Hodges and D. J. Wales, Chem. Phys. Lett. **324**, 279 (2000).
[30] S. J. Singer, S. McDonald, and L. Ojamäe, J. Chem. Phys. **112**, 710 (2000).
[31] H. Kabrede and R. Hentschke, J. Phys. Chem. B **107**, 3914 (2003).
[32] S. MacDonald, L. Ojamäe, and S. J. Singer, J. Phys. Chem. **102**, 2824 (1998); J.-L. Kuo, J. V. Coe, and S. J. Singer, J. Chem. Phys. **114**, 2527 (2001).
[33] G. Zundel and H. Z. Metzger, Z. Phys. Chem. (Munich) **58**, 225 (1968).
[34] Y.-S. Wang, J. C. Jiang, C.-L. Cheng, S. H. Lin, Y. T. Lee, and H.-C. Chang, J. Chem. Phys. **107**, 9695 (1997).
[35] H.-C. Chang, Y.-S. Wang, Y. T. Lee, and H.-C. Chang, Int. J. Mass Spectrom. **179-180**, 91 (1998).
[36] Y.-S. Wang, H.-C. Chang, J.-C. Jiang, S. H. Lin, Y. T. Lee, and H.-C. Chang, J. Am. Chem. Soc. **120**, 8777 (1998).
[37] H. Shinohara, U. Nagashima, and N. Nishi, Chem. Phys. Lett. **111**, 511 (1984); H. Shinohara, U. Nagashima, H. Tanaka, and N. Nishi, J. Chem. Phys. **83**, 4183 (1985); U. Nagashima, N. Nishi, and H. Tanaka, *ibid.* **84**, 209 (1986).
[38] E. G. Diken, N. I. Hammer, M. A. Johnson, R. A. Christie, and K. D. Jordan, J. Chem. Phys. **123**, 164309 (2005).
[39] M. Schmidt, A. Masson, C. Bréchignac, and H. P. Cheng, J. Chem. Phys. **126**, 154315 (2007).
[40] S. G. Lias, J. F. Liebman, and R. D. Levin, J. Phys. Chem. Ref. Data **13**, 695 (1984).
[41] H. P. Cheng, J. Chem. Phys. **105**, 6844 (1996), and references therein.
[42] S. Galera, J. Luch, and J. Bertran, THEOCHEM **163**, 101 (1988).
[43] A. Pullman and A. M. Armbruster, Int. J. Quantum Chem., Symp. **8**, 169 (1974).
[44] P. J. Desmeules and L. C. Allen, J. Chem. Phys. **72**, 4731 (1980).
[45] S. Ikuta, Chem. Phys. Lett. **95**, 604 (1983).
[46] H. J. Böhm and I. R. McDonald, J. Chem. Soc., Faraday Trans. 2 **80**, 887 (1984).
[47] A. Pullman, P. Claverie, and M. C. Cluzan, Chem. Phys. Lett. **117**, 419 (1985).
[48] M. Welti, T. K. Ha, and E. Pretsch, J. Chem. Phys. **83**, 2959 (1985).
[49] C. A. Deakyne, J. Phys. Chem. **90**, 6625 (1986).
[50] E. Kassab, E. M. Evleth, and Z. D. Hamou-Tahra, J. Am. Chem. Soc. **112**, 103 (1990).

[51] A. T. Pudzianowski, J. Chem. Phys. **102**, 8029 (1995).
[52] J. C. Contador, M. A. Aguilar, and F. J. Olivares del Valle, Chem. Phys. **214**, 113 (1997).
[53] S. Karthikeyan, J. T. Singh, M. Park, R. Kumar, and K. S. Kim, J. Chem. Phys. **128**, 244304 (2008).
[54] J. C. Jiang, H.-C. Chang, Y. T. Lee, and S. H. Lin, J. Phys. Chem. A **103**, 3123 (1999).
[55] H. M. Lee, P. Tarakeshwar, J. Park, M. R. Kolaski, Y. J. Yoon, H.-B. Yi, W. Y. Kim, and K. S. Kim, J. Phys. Chem. A **108**, 2949 (2004).
[56] F. C. Pickard IV, M. E. Dunn, and G. C. Shields, J. Phys. Chem. A **109**, 4905 (2005).
[57] A. Khan, Chem. Phys. Lett. **338**, 201 (2001).
[58] J. C. Grossman, E. Schwegler, E. W. Draeger, F. Gygi, and G. Galli, J. Chem. Phys. **120**, 300 (2004).
[59] C. L. Perrin and R. K. Gipe, J. Am. Chem. Soc. **90**, 2174 (1986).
[60] C. L. Perrin and R. K. Gipe, Science **238**, 1393 (1987).
[61] W. L. Jorgensen and J. Gao, J. Phys. Chem. **90**, 2174 (1986).
[62] E. Kassab, E. M. Evleth, and Z. D. Hamous-Tahra, J. Am. Chem. Soc. **112**, 103 (1990).
[63] O. A. Karim and A. D. J. Haymet, J. Chem. Phys. **93**, 5961 (1990).
[64] R. Noto, V. Martorana, M. Migliore, and S. L. Fornili, Z. Naturforsch. Teil A **46**, 107 (1991).
[65] L. X. Dang, Chem. Phys. Lett. **213**, 541 (1993).
[66] F. Brugé, M. Bernasconi, and M. Parrinello, J. Chem. Phys. **110**, 4734 (1999).
[67] J. C. Jiang, H. C. Chang, Y. T. Lee, and S. H. Lin, J. Phys. Chem. **103**, 3123 (1999).
[68] F. Brugé, M. Bernasconi, and M. Parrinello, J. Am. Chem. Soc. **121**, 10883 (1999).
[69] T.-M. Chang and L. X. Dang, J. Chem. Phys. **118**, 8813 (2003).
[70] R. E. Kozack and P. C. Jordan, J. Chem. Phys. **96**, 3120 (1992).
[71] R. E. Kozack and P. C. Jordan, J. Chem. Phys. **96**, 3131 (1992).
[72] J. M. Lisy, Int. Rev. Phys. Chem. **16**, 267 (1997).
[73] C. J. Burnham, S. S. Xantheas, M. A. Miller, B. E. Appligate, and R. E. Miller, J. Chem. Phys. **117**, 1109 (2002).
[74] C. J. Tsai and K. D. Jordan, J. Chem. Phys. **95**, 3850 (1991).
[75] C. J. Tsai and K. D. Jordan, J. Chem. Phys. **99**, 6957 (1993).
[76] A. N. Tharrington and K. D. Jordan, J. Phys. Chem. A **107**, 7380 (2003).
[77] C. Caleman and D. van der Spoel, J. Chem. Phys. **125**, 154508 (2006).
[78] M. J. McGrath, J. I. Siepmann, I. F. W. Kuo, C. J. Mundy, J. VandeVondele, J. Hutter, F. Mohamed, and M. Krack, J. Phys. Chem. A **110**, 640 (2006).
[79] Y. A. Mantz, B. Chen, and G. J. Martyna, J. Phys. Chem. B **110**, 3540 (2006).
[80] S. Shin, W. S. Son, and S. Jang, J. Mol. Struct.: THEOCHEM **673**, 109 (2004).
[81] S. F. Langley, E. Curotto, D. L. Freeman, and J. D. Doll, J. Chem. Phys. **126**, 084506 (2007).
[82] P. A. Frantsuzov and V. A. Mandelshtam, J. Chem. Phys. **128**, 094304 (2008).
[83] U. Buck, I. Ettischer, M. Melzer, V. Buch, and J. Sadlej, Phys. Rev. Lett. **80**, 2578 (1998).
[84] B. Hartke, Z. Phys. Chem. **214**, 1251 (2000).
[85] J. K. Kazimirski and V. Buch, J. Phys. Chem. A **107**, 9762 (2003).
[86] B. Hartke, Phys. Chem. Chem. Phys. **5**, 275 (2003).
[87] T. James, D. J. Wales, and J. Hernández-Rojas, Chem. Phys. Lett. **415**, 302 (2005).
[88] B. Bandow and B. Hartke, J. Phys. Chem. A **110**, 5809 (2006).
[89] G. Geyer, in *Computing Science and Statistics: Proceedings of the 23rd Symposium on the Interface*, edited by E. K. Keramidas (Interface Foundation, Fairfax Station, 1991), p. 156.
[90] A. D. Becke, J. Chem. Phys. **98**, 5648 (1993).
[91] C. Lee, W. Yang, and R. G. Parr, Phys. Rev. B **37**, 785 (1988).
[92] A. D. McLean and G. S. Chandler, J. Chem. Phys. **72**, 5639 (1980).
[93] R. Krishnan, J. S. Binkley, R. Seeger, and J. A. Pople, J. Chem. Phys. **72**, 650 (1980).
[94] T. Clark, J. Chandrasekhar, G. W. Spitznagel, and P. V. R. Schleyer, J. Comput. Chem. **4**, 294 (1983).
[95] M. J. Frisch, J. A. Pople, and J. S. Binkley, J. Chem. Phys. **80**, 3265 (1984).
[96] W. J. Hehre, R. Ditchfield, and J. A. Pople, J. Chem. Phys. **56**, 2257 (1972).
[97] B. Chourabi and J. J. Fripiat, Clays Clay Miner. **29**, 260 (1981).
[98] E. Srasra, F. Bergaya, and J. J. Fripiat, Clays Clay Miner. **42**, 237 (1994).
[99] J. Pironon, M. Pelletier, P. De Donato, and R. Mosser-Ruck, Clays Clay Miner. **38**, 201 (2003).
[100] J. Kim, S. Lee, S. J. Cho, B. J. Mhin, and K. S. Kim, J. Chem. Phys. **102**, 839 (1995).
[101] K. S. Kim, P. Tarakeshwar, and J. Y. Lee, Chem. Rev. (Washington, D.C.) **100**, 4145 (2000).
[102] S. F. Boys and F. Bernardi, Mol. Phys. **19**, 553 (1970).
[103] M. J. Frisch, G. W. Trucks, H. B. Schlegel *et al.*, GAUSSIAN 03, Revision C.02, Gaussian, Inc., Wallingford CT, 2004.
[104] F. Calvo, J. P. K. Doye, and D. J. Wales, J. Chem. Phys. **114**, 7312 (2001).
[105] F. Calvo, J. P. K. Doye, and D. J. Wales, Chem. Phys. Lett. **366**, 176 (2002).
[106] S. F. Chekmarev and S. V. Krivov, Phys. Rev. E **57**, 2445 (1998).
[107] T. V. Bogdan, D. J. Wales, and F. Calvo, J. Chem. Phys. **124**, 044102 (2006).
[108] F. Calvo, J. P. K. Doye, and D. J. Wales, J. Chem. Phys. **115**, 9627 (2001).
[109] V. Barone, J. Chem. Phys. **122**, 014108 (2005).
[110] S. Kumar, D. Bouzida, R. H. Swendsen, P. A. Kollman, and J. M. Rosenberg, J. Comput. Chem. **13**, 1011 (1992).
[111] B. G. Johnson, P. M. W. Gill, and J. A. Pople, J. Chem. Phys. **98**, 5612 (1993).
[112] M. P. Andersson and P. Uvdal, J. Phys. Chem. A **109**, 2937 (2005).
[113] F. Weigend and M. Häser, Theor. Chem. Acc. **97**, 331 (1997).
[114] F. Weigend, M. Häser, H. Patzelt, and R. Ahlrichs, Chem. Phys. Lett. **294**, 143 (1998).
[115] T. H. Dunning, Jr., J. Chem. Phys. **90**, 1007 (1989).
[116] R. A. Kendall, T. H. Dunning, Jr., and R. J. Harrison, J. Chem. Phys. **96**, 6796 (1992).
[117] K. D. Jordan, private communication (June 2008).
[118] G. K. Schenter, S. M. Kathmann, and B. C. Garrett, Phys. Rev. Lett. **82**, 3484 (1999); J. Chem. Phys. **110**, 7951 (1999); S. M. Kathmann, G. K. Schenter, and B. C. Garrett, *ibid.* **111**, 4688 (1999); **116**, 5046 (2002); **120**, 9133 (2004); S. M. Kathmann, B. J. Palmer, G. K. Schenter, and B. C. Garrett, *ibid.* **128**, 064306 (2008).
[119] P. Pechukas and J. C. Light, J. Chem. Phys. **42**, 3281 (1965); J. Lin and J. C. Light, *ibid.* **43**, 3209 (1965); E. Nikitin, Theor. Exp. Chem. **1**, 83 (1965); **1**, 90 (1965); **1**, 275 (1965); C. E. Klots, J. Phys. Chem. **75**, 1526 (1971); Z. Naturforsch. A **27**, 553 (1971); Adv. Mass Spectrom. **6**, 9696 (1973); W. J. Chesnavich and M. T. Bowers, J. Am. Chem. Soc. **98**, 8301 (1976); J. Chem. Phys. **66**, 2306 (1977); J. Am. Chem. Soc. **99**, 1705 (1977); F. Calvo and P. Parneix, J. Chem. Phys. **119**, 256 (2003); **120**, 2780 (2004).